Batch and continuous processes for the removal of Al3+ and Fe2+ from aqueous effluents using spent coffee ground

Processos batch e contínuo para a remoção de Al3+ e Fe2+ de efluentes aquosos utilizando café moído

DOI: 10.46814/lajdv4n3-039

Recebimento dos originais: 31/03/2022
Aceitação para publicação: 18/04/2022

Silvio José Valadão Vicente
Doutor em Saúde Pública
Institution: Universidade Santa Cecília
Address: R. Oswaldo Cruz, 266, Santos-SP, Brasil
E-mail: laq@unisanta.br

Ana Caroline da Silva Gonçalves Aluoto
Engenheira Química
Institution: Universidade Santa Cecília
Address: R. Oswaldo Cruz, 266, Santos-SP, Brasil
E-mail: acsilva@brssz.com

Diego Armando Santos Alves
Mestre em Engenharia Química
Institution: Universidade Santa Cecília
Address: R. Oswaldo Cruz, 266, Santos-SP, Brasil
E-mail: diegoarmando.alves@gmail.com

Lidiane Fernandes Bueno
Engenheira Química
Institution: Universidade Santa Cecília
Address: R. Oswaldo Cruz, 266, Santos-SP, Brasil
E-mail: lidiane.fb@hotmail.com

Luisa de Oliveira Pinto Francisco
Engenheira Química
Institution: Universidade Santa Cecília
Address: R. Oswaldo Cruz, 266, Santos-SP, Brasil
E-mail: luisaopf@gmail.com

Victor Basile Astuto
Engenheiro Químico
Institution: Universidade Santa Cecília
Address: R. Oswaldo Cruz, 266, Santos-SP, Brasil
E-mail: vastuto@iq.usp.br

ABSTRACT
Due to the intense industrialization of the modern society, severe contamination of water by dangerous metal ions has become a major problem. The use of plant-derived biosorbents has been proposed in

different studies in reason of their good performance and marginal cost. The proposal of this study was to evaluate the use of spent coffee ground (SCG) for the removal of metal ions from aqueous effluents. The batch process showed removal efficiencies equal to 92.4% for Al^{3+} and 85.9% for Fe^{2+}, and the continuous process showed removal efficiencies equal to 97.2% for Al^{3+} and 96.2% for Fe^{2+}. These two processes were compared using Freundlich and Langmuir models, and Langmuir-3 model showed the best adequacy for all processes indicating to be favorable ($0.12 \leq R_L \leq 0.59$), with equilibrium sorption capacities between 1.79 and 4.21 mg/g SCG. Kinetic evaluations suggested that these two processes follow a pseudo-second order model for both ions, with thermodynamically favorable characteristics. All data indicated that this biosorbent has a good potential to be used for the removal of metal ions from contaminated aqueous effluents.

Keywords: coffee, sorption, metal ions, isotherm, kinetics.

RESUMO

Devido à intensa industrialização da sociedade moderna, a grave contaminação da água por íons metálicos perigosos tornou-se um grande problema. O uso de bioorbentes derivados de plantas tem sido proposto em diferentes estudos em razão de seu bom desempenho e custo marginal. A proposta deste estudo foi avaliar o uso de café moído (SCG) gasto para a remoção de íons metálicos de efluentes aquosos. O processo em lote mostrou eficiências de remoção iguais a 92,4% para Al3+ e 85,9% para Fe2+, e o processo contínuo mostrou eficiências de remoção iguais a 97,2% para Al3+ e 96,2% para Fe2+. Estes dois processos foram comparados utilizando os modelos Freundlich e Langmuir, e o modelo Langmuir-3 mostrou a melhor adequação para todos os processos indicando ser favorável (0,12 ≤ RL ≤ 0,59), com capacidades de sorção de equilíbrio entre 1,79 e 4,21 mg/g SCG. As avaliações cinéticas sugeriram que estes dois processos seguem um modelo de ordem pseudo-segunda para ambos os íons, com características termodinamicamente favoráveis. Todos os dados indicam que este biosorbente tem um bom potencial para ser utilizado para a remoção de íons metálicos de efluentes aquosos contaminados.

Palavras-chave: café, sorção, íons metálicos, isoterma, cinética.

1 INTRODUCTION

Water contamination by heavy metals has been identified as one of the most serious environmental problems in the world (Dávila-Guzmán et al., 2013; Vijayaraghavan and Balasubramanian, 2015). Some of these components are beneficial for life, acting as essential micronutrients. However, the accumulation of metal ions in water and subsequent excessive absorption by living organisms, including humans, results in detrimental health effects. For this reason, the removal of these contaminants from the water has become a major issue (Hashim et al., 2011).

The earth's crust contains hundreds of minerals that present metal ions in their compositions. A small quantity of these ions is naturally dissolved into groundwater with no consequences (Hashim et al., 2011). However, increasingly needs of manufactured goods and agricultural foodstuffs have been generating unprecedented volumes of industrial and rural effluents containing high concentrations of metal ions, contaminating soil and groundwater (Agbozu & Emoruwa, 2014; Vijayaraghavan and

Balasubramanian, 2015). Mining, metal plating, fertilizers and pesticides production and utilization, batteries manufacturing, painting, chloralkali plants, textile, tanneries and alloy industries are the main sources of contaminations related to heavy metals (Agbozu & Emoruwa, 2014; Wang et al., 2019; Vijayaraghavan and Balasubramanian, 2015). Taking into account that metal ions are not biodegradable, they accumulate in water and soil being absorbed by life forms, resulting in diseases, biological disorders and death (Agbozu & Emoruwa, 2014.; Revathi et al., 2012; Sathasivam & Haris, 2010). For humans, the extreme toxicity of some heavy metals can impair mental functions and cause damages to the lungs, liver, blood composition, brain, kidneys and reproductive system (Amarasinghe & Williams, 2007; Sathasivam & Haris, 2010).

Different chemical and physical methods have been proposed to reduce the concentration of these aggressors, each one showing merits and disadvantages. The latest technologies include ion exchange (extremely expensive), activated carbon adsorption (frequent high cost regeneration), uptake by microorganisms (production of highly contaminated biological residues), chemical precipitation (poor efficiency at low concentrations), electrochemical deposition (production of large amounts of contaminated sludge), and membrane technologies (frequent clogging and expensive regeneration) among others (Hashim et al, 2011; Keng et al, 2014; Vijayaraghavan and Balasubramanian, 2015; Witek-Krowiak et al., 2011).

Studies have been suggesting that sorption processes based on plant-derived residues from agro-industrial activities should be considered as interesting alternatives for the removal of metal ions from aqueous effluents. Different low-priced, quite efficient and largely available biosorbents such as pinewood sawdust, coconut shell, rice husks, peanut shell, orange bark, olive oil waste, wheat bran, corncob and watermelon rind have been confirmed to exhibit sorption properties for metal ions (Amarasinghe & Williams, 2007; Azouaou et al., 2010; Lakshmipathy & Sarada, 2013; Souza et al., 2010). Different mathematical approaches have been proposed to quantify the efficiency of these sorption processes and the models developed by Langmuir and Freundlich are frequently used (Azouaou et al, 2010; Vijayaraghavan and Balasubramanian, 2015; Wang et al., 2017).

The Langmuir model proposes that the sorption occurs in a single layer, which is uniform, simple, infinite and non-leaky (Langmuir, 1916; Vijayaraghavan and Balasubramanian, 2015;). This model follows the equation

$$Q_e = (Q_m.K_L.C_e)/(1+K_L.C_e) \qquad (1)$$

where Q_e is the sorption capacity at the equilibrium point, Q_m is the maximum sorption capacity, K_L is the Langmuir constant related to sorption free energy and C_e is the unabsorbed concentration at

the equilibrium point.

The dimensionless equilibrium parameter R_L can be used to predict the favorability of the process. When $R_L > 1$, the process is unfavorable; when $R_L = 1$, the process is linear; when $0 < R_L < 1$, the process is favorable and when $R_L = 0$, the process is irreversible (Wang et al., 2019). The calculation of R_L can be done using the equation

$$R_L = 1/(1+K_L.Q_m) \qquad (2)$$

The Freundlich model is also extensively used and it assumes that the sorption process occurs according to a multilayer event (Freundlich, 1906) that has irregular sites with different energies of absorption (Sathasivam & Haris, 2010). This model admits a logarithm distribution of the active sites and a highly heterogeneous sorption surface. The sorption capacity is determined by the equation

$$Q_e = K_F.C_e^{1/n} \qquad (3)$$

where K_F is the Freundlich constant related to the sorption capacity and n is the Freundlich exponent related to the efficiency of the process. According to this model, when $2 < n < 10$ the process is favorable.

To make the use of these two models easier, they can be applied using their linearized equations exhibited in Table 1.

Table 1 Linearized equations of Langmuir and Freundlich models.

Isotherm model	Linear equation		Graph
Langmuir-1	$C_e/Q_e = (1/Q_m).C_e + 1/(K_L.Q_m)$	(4)	C_e/Q_e x C_e
Langmuir-2	$1/Q_e = 1/(K_L.Q_m).(1/C_e) + 1/Q_m$	(5)	$1/Q_e$ x $1/C_e$
Langmuir-3	$Q_e = Q_m - (1/K_L).(Q_e/C_e)$	(6)	Q_e x Q_e/C_e
Langmuir-4	$Q_e/C_e = (K_L.Q_m) - (K_L.Q_e)$	(7)	Q_e/C_e x Q_e
Freundlich	$\log Q_e = \log K_F + (1/n).\log C_e$	(8)	$\log Q_e$ x $\log C_e$

Because the Langmuir model has four different linearized equations, the sum of squares (ss) method can be used to identify which of these options is more adequate to fit the experimental results (Muslin et al., 2022). The ss method is also useful to compare Langmuir and Freundlich models to check which one is more satisfactory in analyzing the results.

Additional information including the uptake rate during sorption processes can be obtained through kinetic evaluations, and two models are often used. The pseudo-first order model (Gao et al., 2016) is represented by the equation

$$\log (Q_e - Q_t) = \log Q_e - (k_1/2.303).t \quad (9)$$

where Q_t is the quantity of solute absorbed at a time t and k_1 is the pseudo-first order velocity constant. The other option is the pseudo-second order model (Gao et al., 2016), which is expressed by the equation

$$t/Q_t = 1/(k_2.Q_{e2}) + (t/Q_e) \quad (10)$$

where k_2 is the pseudo-second order velocity constant.

In view of the above information, this study evaluated the use of spent coffee ground (SCG) as biosorbent for the removal of metal ions from aqueous solutions. Batch and continuous processes were tested for Al^{3+} and Fe^{2+}, making possible the comparison between their removal efficiencies.

2 MATERIALS AND METHODS

2.1 SPENT COFFEE GROUND PREPARATION

SCG was collected right after generation in different coffee shops of the university, all attended by the same coffee powder supplier. The material was washed with distilled water and sifted to a particle size > 0.18 mm (80-mesh screen). Next, the SCG was dried at 105 ± 5 °C for 5 hours and stored in dark glass containers until use. Prior to the use, the humidity of the SCG was determined (Ahn et al., 2019).

2.2 METHODS

2.2.1 Surface structure and FTIR spectral analysis

The SCG surface structure was investigated by scanning electron microscopy (SEM) using an equipment supplied by JEOL (Japan) model JSM-7401F, operating at 3.0 kV. The identification of surface functional groups was done by Fourier Transform Infrared (FTIR) using a spectrophotometer supplied by Perkin Elmer (USA) model Frontier, with 4 cm^{-1} resolution and 32 cumulative scans (KBr pellets, 1% wt/wt).

2.2.2 Spectrophotometric analysis

The quantification of Fe^{2+} was done according to the method 3500-Fe B (phenanthroline method) described in the Standard Methods for the Examination of Water and Wastewater (Baird et al., 2017). The calibration curve was obtained using Fe^{2+} solutions ranging from 1.0 to 20.0 mg/L and the measurements were done at 510 nm. The quantification of Al^{3+} was done according to the same

reference (Baird et al., 2017) using the method 3500-Al B (eriochrome cyanine R method). A calibration curve was prepared using Al^{3+} solutions ranging from 1.0 to 20.0 mg/L and the tests were performed at 535 nm.

2.2.3 Continuous tests

The equipment used for the continuous tests included an acrylic column (40.0 x 4.5 cm) equipped with a precision glass valve in the bottom and a 250 mL separating funnel on the top. Initially, the desired mass of SCG was loaded into the column followed by 320 mL of a solution with the desired concentration of Fe^{2+} or Al^{3+}, resulting in a 20-cm liquid level (care was taken to avoid the formation of preferential channels). Then, the desired flow was adjusted with the aid of the glass valve. To keep the flow steady, the valve of the separating funnel was adjusted to keep the 20-cm level constant. Five hundred mL of the testing solution was percolated in each test and the flow was periodically checked using a calibrated measuring cylinder and a chronometer. After the percolation of 500 mL, the remaining Fe^{2+} or Al^{3+} was determined in the treated solution. The parameters contact time (min) and mass of SCG (g) were evaluated to find the optimum conditions for the continuous process. All tests were done at 20 ± 3 °C and the SCG used in the tests was discarded.

2.2.4 Batch tests

For the batch tests, the desired mass of SCG was transferred to a 1.0 liter jar test container followed by 500 mL of a solution containing the desired concentration of Fe^{2+} or Al^{3+} (care was taken to avoid the formation of lumps). Next, the mechanical agitation (flat blade impeller, 8.0 x 2.5 cm) was turned on at the desired speed. After the test, the SCG was filtered (quantitative paper filter, 80 g/m^2) and the remaining Fe^{2+} or Al^{3+} was quantified in the treated solution. Prior to these tests, solutions with 2.0 and 20.0 mg/L of Fe^{2+} or Al^{3+} were filtered through the selected paper filter and no reduction in the ions concentrations were observed. The parameters time of agitation (min), agitation speed (rpm) and mass of SCG (g) were evaluated to identify the optimum conditions for the batch process. All tests were done at 20 ± 3 °C and the SCG used in the tests was discarded.

2.3 STATISTICAL ANALYSIS

The Shapiro-Wilk test was applied for testing the normality of samples. The Student's t test was applied using the software SPSS - Statistical Package for the Social Science software version 16.0 for Windows, with a significance level of $p < 0.05$. All analyses were carried out in triplicate and the results are expressed as average ± standard deviation.

3 RESULTS AND DISCUSSION

3.1 SCG CHARACTERIZATION

After washing, sifting and drying, the SCG was analyzed and the main results were particle size larger than 0.18 mm, moisture between 1.6 and 2.2% (wt/wt) depending on the drying step and ash content between 1.89 and 2.02% (wt/wt).

The sorption capacity of a biosorbent is normally associated to the existence of high polarity groups on its surface. These groups are able to create negative net charges, forming binding sites capable of exerting electrostatic attraction to positive metal ions present in aqueous solutions (Azouaou et al., 2010; Chao et al., 2014; Dávila-Gusmán et al., 2013). To confirm the existence of these polar groups in the SCG, a FTIR spectrum was obtained (Figure 1).

Fig. 1. Infrared spectrum of the SCG showing the presence of different polar groups.

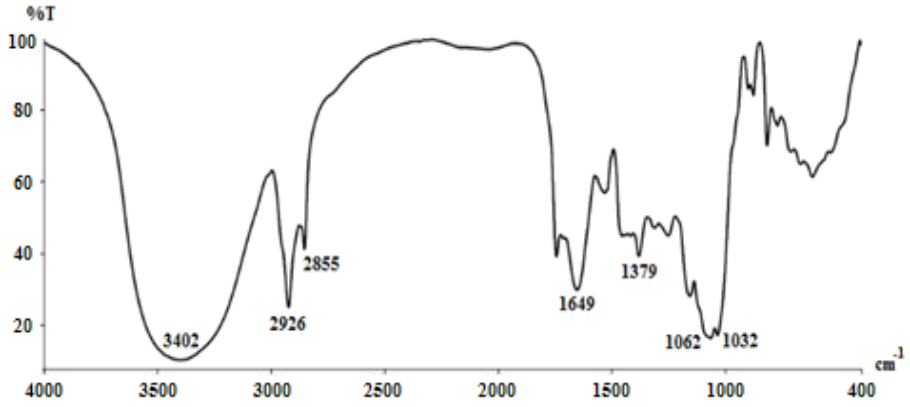

The more important bands identified in this spectrum were 3402 cm^{-1} (O-H and/or COOH stretching), 2926 and 2855 cm^{-1} (symmetric and asymmetric stretching of aliphatic C-H), 1649 cm^{-1} (C=O and/or COO^- groups), 1379 cm^{-1} (COO^- stretching) and 1062 and 1032 cm^{-1} (S=O and/or carbohydrate groups) (Azouaou et al., 2010; Chao et al., 2014; Dávila-Gusmán et al., 2013). Therefore, the presence of high polarity groups were confirmed, suggesting that SCG can be a candidate for sorption processes.

In addition to FTIR, the morphology of SCG surface was investigated by SEM at different magnifications (Figure 2). Picture A obtained at 3.0 kV and x250 magnification shows that SCG has a homogeneous and porous texture with abundant valleys and peeks, exhibiting an intermediate roughness. Picture B obtained at 3.0 kV and x3,500 magnification shows that SCG has a macroporous structure, with an average pore diameter of around 10 μm. This pore size is large enough to accommodate the metal ions used in the present study (Al^{3+} = 0.51 Å; Fe^{2+} = 0.74 Å).

Fig. 2. SEM images of SCG (WD 8.0 mm, 3.0 kV).

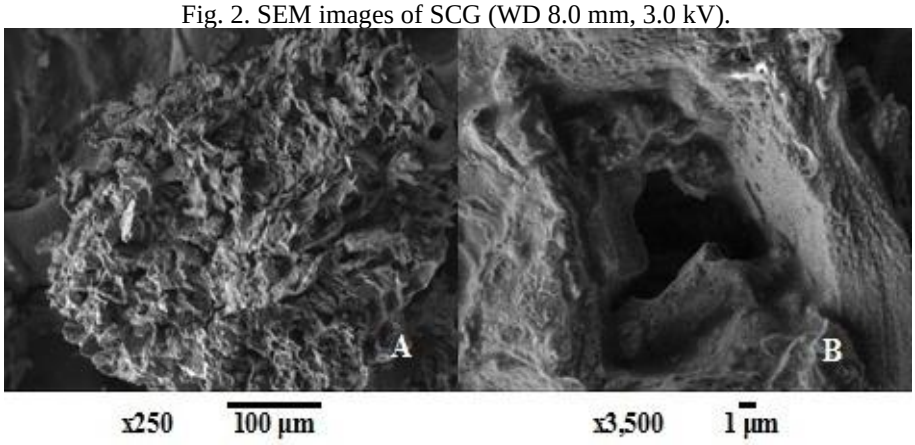

3.2 COMPARISON BETWEEN BATCH AND CONTINUOUS PROCESSES FOR AL^{3+}

This study was initiated by evaluating the removal of Al^{3+} from aqueous solutions using the batch process. In the first sequence, the parameters mass of SCG and agitation speed were arbitrarily fixed in 5.0 g (dry matter) and 60 rpm, respectively. The SCG and 500 mL of solution with 20 mg/L Al^{3+} were loaded into the jar test container, the agitation was turned on and the time of agitation was varied from 10 to 80 min. At the end of each test, the remaining Al^{3+} was determined by visible spectroscopy and the removal efficiency versus time of agitation was plotted (graph not included) showing that after 60 min, the efficiency reached 77.5%. As longer runs did not increase significantly this value, the optimum agitation time was defined as 60 min.

Next, the agitation time was fixed in 60 min (as determined), the mass of SCG was arbitrarily fixed in 5.0 g and the agitation speed was changed from 40 to 140 rpm. After the tests, the removal efficiency versus agitation speed was plotted (graph not included) showing that the efficiency rapidly increased from 0 to 50 rpm and then started to stabilize, reaching 91.1% at 80 rpm with no significant increase using faster agitation. Therefore, the efficient agitation speed was fixed in 80 rpm.

In the last sequence, the agitation time and agitation speed were fixed in 60 min and 80 rpm (as determined), and the mass of SCG was changed from 0 to 12.0 g. Removal efficiency versus mass of SCG reached 92.4% using 7.5 g of SCG and no significant gain was obtained by increasing the mass of biosorbent (Figure 3). After these tests, it was possible to conclude that 92.4% would be the efficiency limit for the batch process taking into account the tested ranges.

After finishing the batch process, the continuous tests for Al^{3+} were initiated. In the first sequence, the mass of SCG was arbitrarily fixed in 5.0 g (dry matter) and the elution time through the column was studied from 0 to 11 min. During the tests, a rapid and almost linear increase of the removal efficiency was observed from 0 to 5 min that started to stabilize using longer elution time, reaching 78.1% after 9 min of elution (graph not included). As longer runs did not result in greater efficiency, 9 min was defined as the optimum elution time.

Then, the variable mass of SCG was evaluated from 0 to 12.0 g, keeping the elution time equals to 9 min (as determined). As shown in Figure 3, removal efficiency increased rapidly from 0 to 6.0 g of SCG, starting to stabilize with larger quantities of biosorbent. Using 7.5 g of SCG, the removal efficiency reached 97.2% that was assumed as the efficiency limit for the continuous process taking into account the tested ranges.

Fig. 3. Comparison between batch and continuous processes for the removal of Al^{3+} from aqueous solutions (n = 3). The points marked with * are statistically not different from the efficiency limits ($p \leq 0.05$).

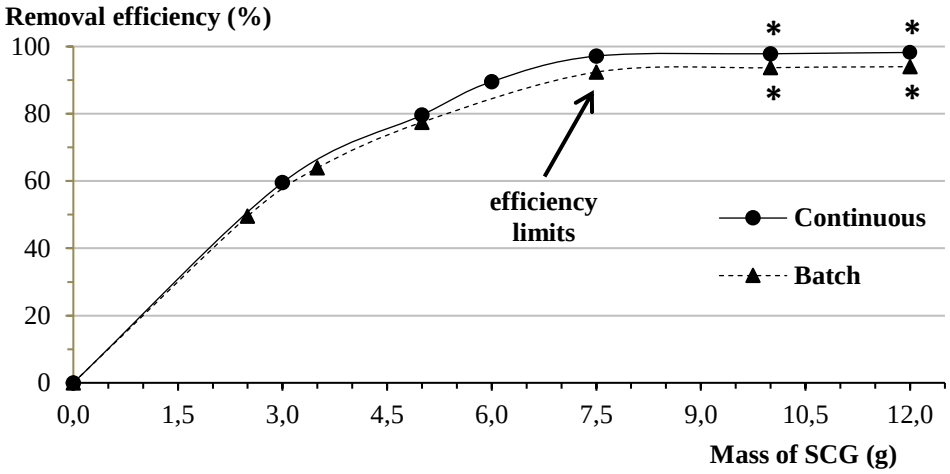

3.3 COMPARISON BETWEEN BATCH AND CONTINUOUS PROCESSES FOR FE^{2+}

After finishing the tests for Al^{3+} and using the acquired knowledge, equivalent experiments were done for Fe^{2+} starting with the batch process. In the first sequence, the mass of SCG was fixed in 5.0 g (dry matter) and the agitation speed was fixed in 60 rpm. Then, the SCG and 500 mL of solutions containing 20 mg/L Fe^{2+} were loaded into the jar test container and agitated for periods ranging from 10 to 90 min. The graph of these results (not included) indicated that after 60 min, the removal efficiency reached 84.2% and additional agitation time did not increase the effectiveness of the process and for this reason, the optimal agitation time was fixed in 60 min.

Subsequently, the influence of agitation was evaluated using 5 g of SCG and 60 min of agitation time (as determined). The agitation speed was varied from 40 to 140 rpm, showing that the removal efficiency rapidly increased until 60 rpm and then started to stabilize reaching 85.6% at 80 rpm with no significant increase under faster agitation. Therefore, the optimum agitation speed was fixed in 80 rpm.

Finally, the effect of the mass of SCG in the batch process was evaluated. Using 60 min as agitation time and 80 rpm as agitation speed (as determined), the mass of biosorbent was varied between 0 and 10.0 g. The removal efficiency reach 85.9% using 7.5 g of SCG and no significant

improvement was obtained with larger mass of biosorbent. This suggested that 85.9% would be the efficiency limit for the batch process within the tested ranges (Figure 4).

After concluding the batch tests for Fe^{2+}, the continuous process was evaluated using solutions containing 20 mg/L of this metal ion. During the first set of experiments, the mass of biosorbent was arbitrarily fixed in 5.0 g and the time of percolation was studied from 0 to 9 min. During these tests, the removal efficiency rapidly increased from 0 to 3 min (graph not included) and after that, the efficiency started to stabilize reaching 91.2% after 5 min of contact. As longer runs did not result in better results, 5 min was defined as the optimum elution time.

Finally, the mass of biosorbent was varied from 0 to 10.0 g keeping 5 min as elution time (as determined). As shown in Figure 4, the removal efficiency rapidly increased from 0 to 3.0 g of SCG, starting to stabilize with the use of larger mass of biosorbent. According to the mentioned figure, the efficiency limit for this process was 96.2% using 7.5 g of SCG.

Fig. 4. Comparison between batch and continuous processes for the removal of Fe^{2+} from aqueous solutions (n = 3). The points marked with * are statistically not different from the efficiency limits ($p \leq 0.05$).

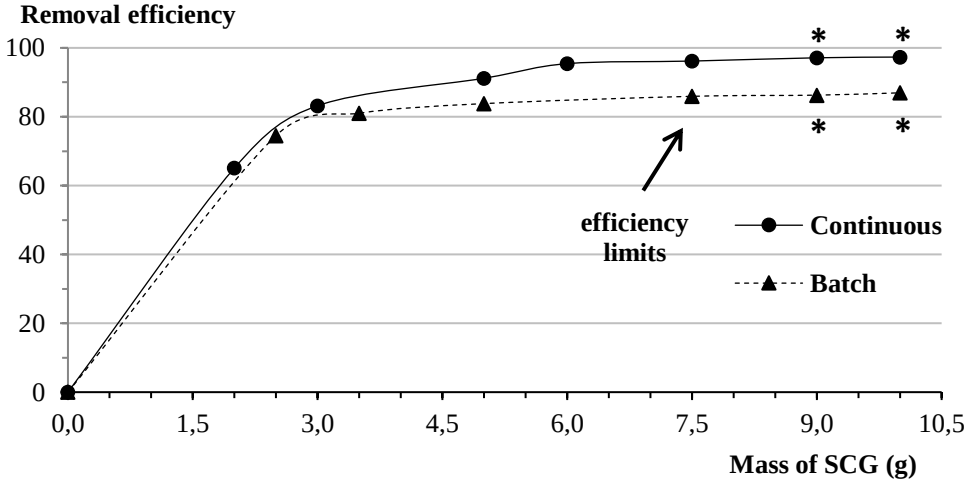

The optimum experimental conditions determined in items 3.2. and 3.3. were then used in item 3.4. tests (isotherm analyzes).

3.4 ISOTHERM ANALYZES

As the Langmuir model has four linearized equations, for better readability only the experimental curve, the best Langmuir theoretical curve (with the lowest value of ss) and the Freundlich theoretical curve were included in the graphs of this item.

3.4.1 Batch process for Al^{3+}

After analyzing the results for the sorption of Al^{3+} using the batch process, it was possible to conclude that Langmuir-3 exhibited the best adequacy to the experimental results. This conclusion based on the visual analysis of the Figure 5 was confirmed by the calculation of ss for each model (ss = 0.072 for Langmuir-3; ss = 0.212 for Freundlich). Therefore, there are evidences that this sorption occurs in a single and uniform layer on SCG surface. Using Langmuir-3 equation and solutions ranging from 0 to 100 mg/L Al^{3+}, the values of K_L (0.91 L/mg Al^{3+}) and Q_m (3.12 mg Al^{3+}/g SCG) were obtained, allowing to the calculation of R_L (0.26) and this value indicated that the thermodynamics of this process is very favorable.

Fig. 5. Experimental and theoretical values for the sorption of Al^{3+} in SCG using the batch process (n = 3).

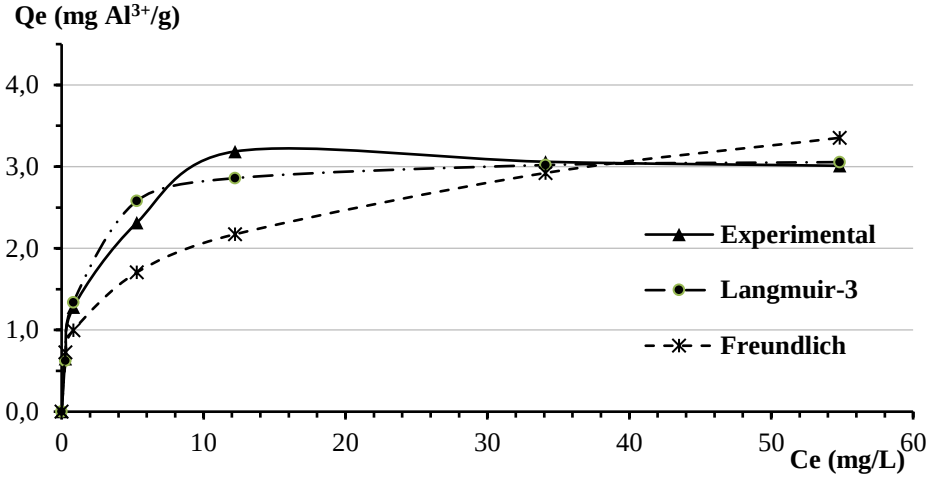

3.4.2 Batch process for Fe^{2+}

The sorption of Fe^{2+} in SCG was also best described by the Langmuir-3 model (ss = 0.077) compared to the Freundlich model (ss = 0.105), as shown in Figure 6. Similar to Al^{3+}, there are evidences that this sorption also occurs in a single and uniform layer. Using different solutions of Fe^{2+} (from 0 to 100 mg/L), the values of Q_m (4.21 mg Fe^{2+}/g SCG), K_L (0.17 L/mg Al^{3+}) and R_L (0.59) were calculated, allowing to conclude that this process is also thermodynamically favorable.

Fig. 6. Experimental and theoretical values for the sorption of Fe^{2+} in SCG using the batch process (n = 3).

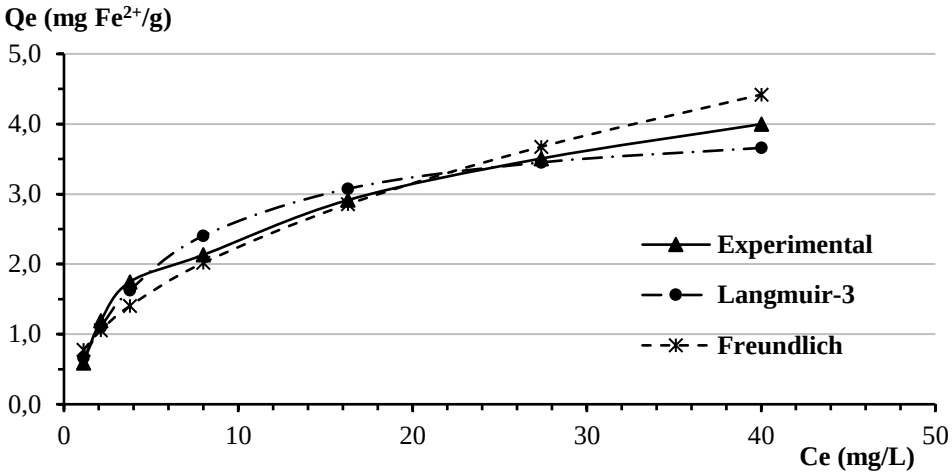

At this point, the comparison of the batch process regarding the sorption of Al^{3+} and Fe^{2+} in SCG was possible and the following conclusions were obtained.

1) The values obtained for R_L showed that the batch process is favorable for both ions. However, Fe^{2+} exhibited a higher value of R_L (ratio R_L Fe^{2+}/R_L Al^{3+} = 2.27) and this suggests that Al^{3+} has a more favorable sorption in SCG.

2) Possible factors to support the previous statement include the ionic radius (Al^{3+} = 0.51 Å; Fe^{2+} = 0.74 Å) and ions charge. These two factors combined suggest a stronger interaction between Al^{3+}/SCG than between Fe^{2+}/SCG, leading to a better accommodation of Al^{3+} into SCG pores.

3) On the other hand, Q_m showed to be 35% higher for Fe^{2+} (Q_m Fe^{2+}/Q_m Al^{3+} = 1.35) showing that SCG can absorb more Fe^{2+} than Al^{3+} per mass unit. The higher charge of Al^{3+} probably creates strong electric/magnetic fields around the complex ion-sorbent, making more difficult to accommodate subsequent ions in the neighborhood, thus reducing the capacity to absorb additional Al^{3+} ions. Besides, Fe^{2+} is approximately two times heavier than Al^{3+} (atomic weights 55.85 and 26.98 respectively), being easier to absorb a larger mass of Fe^{2+} per SCG mass unit.

4) Another possible argument for the previous paragraph involves the constant K_L. This parameter is related to the sorption free energy and Al^{3+} presented a much higher value of K_L (ratio K_L Al^{3+}/K_L Fe^{2+} = 5.45). Considering that the smaller is the free energy, the more spontaneous the process tends to be, it is reasonable to understand the higher value of Q_m for Fe^{2+}.

5) To complete this discussion, it is also interesting to consider the dehydration enthalpy (ΔH_{dehyd}). The higher is ΔH_{dehyd}, the more difficult is to remove the water molecules that are solvating the metal ion to promote a more efficient sorbent-metal ion interaction (Amarasinghe & Williams, 2007). Given that $\Delta H_{dehyd\ Fe2+}$ (1946 kJ/mol) is much lower than $\Delta H_{dehyd\ Al3+}$ (4665 kJ/mol) as published by Smith (1977), the dehydration of Fe^{2+} that precedes the sorption reaction is thermodynamically more

favorable. This agrees with the conclusion of the preceding paragraph, obtained through the values of K_L.

3.4.3 Continuous process for Al^{3+}

Next, the characteristics of the continuous process for the sorption of Al^{3+} in SCG were analyzed. The plot of the experimental data compared to the values predicted by the Langmuir-3 and Freundlich models indicated good agreement as shown in Figure 7, however Langmuir-3 (ss = 0.020) showed better adequacy than Freundlich (ss = 0.080). Similar to the batch process, these experiments indicated that the sorption of Al^{3+} using a continuous process also occurs in a single and uniform layer. Using Langmuir-3 equation, the calculations indicated that Q_m was equal to 1.79 mg Al^{3+}/g SCG and K_L was equal to 3.99 L/mg Al^{3+}, being possible to determine that R_L = 0.12. These results permitted to conclude that the thermodynamics of this process is very favorable.

Fig. 7. Experimental and theoretical values for the sorption of Al^{3+} in SCG using the continuous process (n = 3).

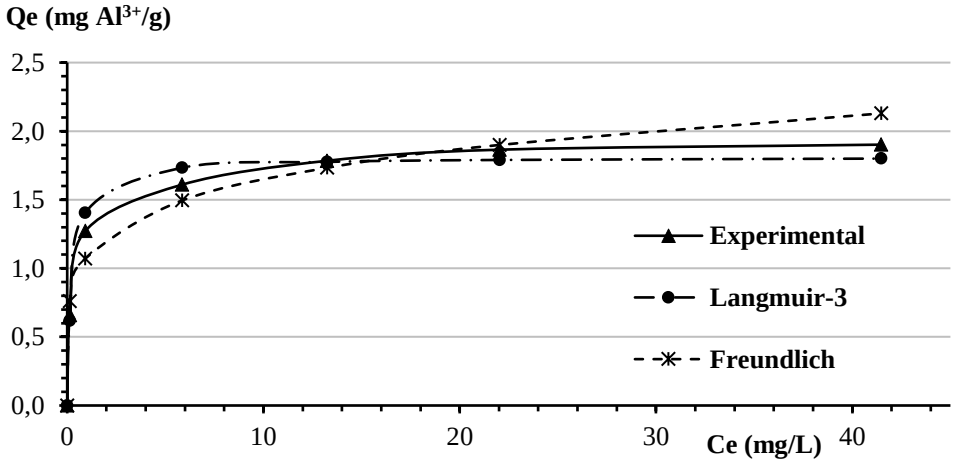

3.4.4 Continuous process for Fe^{2+}

Finally, the continuous process was evaluated to remove Fe^{2+} from aqueous effluents. Once again, the models Langmuir-3 and Freundlich provided good adequacy in relation to the experimental results (ss = 0.066 for Langmuir-3; ss = 0.076 for Freundlich), as shown in Figure 8. Using the Langmuir-3 equation, the values Q_m = 3.34 mg/g SCG and K_L = 0.77 L/mg Al^{3+} were determined, resulting in R_L = 0.28 (thermodynamically very favorable).

Fig. 8. Experimental and theoretical values for the sorption of Fe^{2+} in SCG using the continuous process (n = 3).

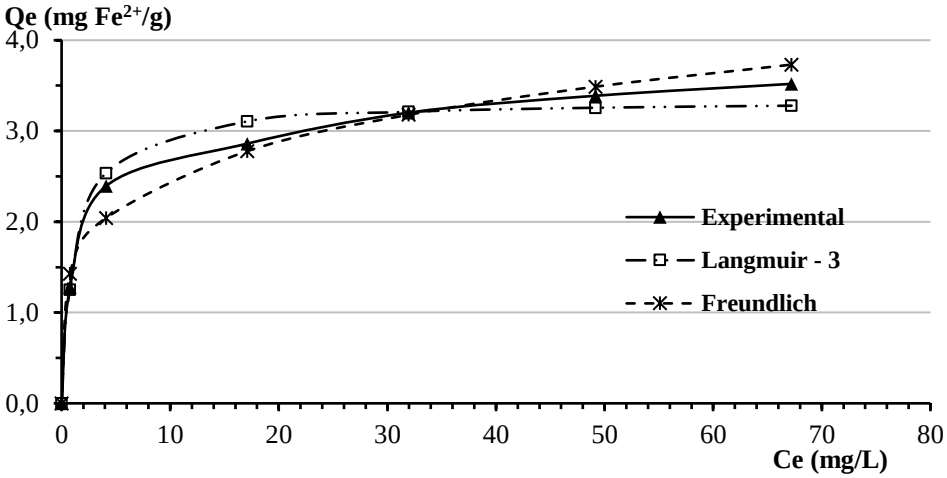

The comparison of the continuous process regarding the sorption of Al^{3+} and Fe^{2+} was also done, and the following conclusions were obtained:

1) The values of R_L show that the continuous process is favorable for both ions. However and in agreement with the batch process, Fe^{2+} showed a higher value of R_L (ratio R_L Fe^{2+}/R_L Al^{3+} = 2.33) and this indicates that the sorption of Al^{3+} in SCG is more favorable. It is interesting to note that the R_L Fe^{2+}/R_L Al^{3+} ratios are practically the same, regardless of the type of process (2.33 for the continuous process, 2.27 for the batch process).

2) The ionic radius and ions charge already discussed for the batch process are also consistent to justify the better accommodation of Al^{3+} into SCG pores and to support the previous statement.

3) In conformity to the batch process, Q_m showed to be higher for Fe^{2+} (Q_m Fe^{2+}/Q_m Al^{3+} = 1.86) indicating that a larger mass of Fe^{2+} can be absorbed per mass unit of SCG. Again, the higher charge of Al^{3+} and the heavier atomic weight of Fe^{2+} are valid arguments to justify this item.

4) Once more, the constant K_L can be used to support the finds related to Q_m. Similar to the batch process, Al^{3+} presented a much higher value of K_L (ratio K_L Al^{3+}/K_L Fe^{2+} = 5.20) justifying the fact that it is possible to absorb a larger mass of Fe^{2+} per mass unit of SCG (lower sorption free energy). Again, the K_L Al^{3+}/K_L Fe^{2+} ratios are similar independent of the type of process (5.20 for the continuous process, 5.45 for the batch process).

5) The discussion about dehydration enthalpy included for batch process is also applicable to justify the reason for Q_m Fe^{2+} > Q_m Al^{3+} for the continuous process.

3.5 SORPTION KINETICS

The sorption kinetics of each process was evaluated starting with the batch process for Al^{3+}. Tests showed a high sorption rate at the beginning of the experiments (high driving force due to the

difference between internal and external concentrations of Al^{3+}), tending to reduce rapidly to reach the equilibrium. The graph log $[(Q_e-Q_t)/Q_e]$ versus time was obtained using the pseudo-first order equation (Figure 9) and the experimental points presented good correspondence to this linear model (R^2 = 0.9599).

Fig. 9. Graph of the experimental data (batch process for Al^{3+}) according to the pseudo-first order equation (n = 3).

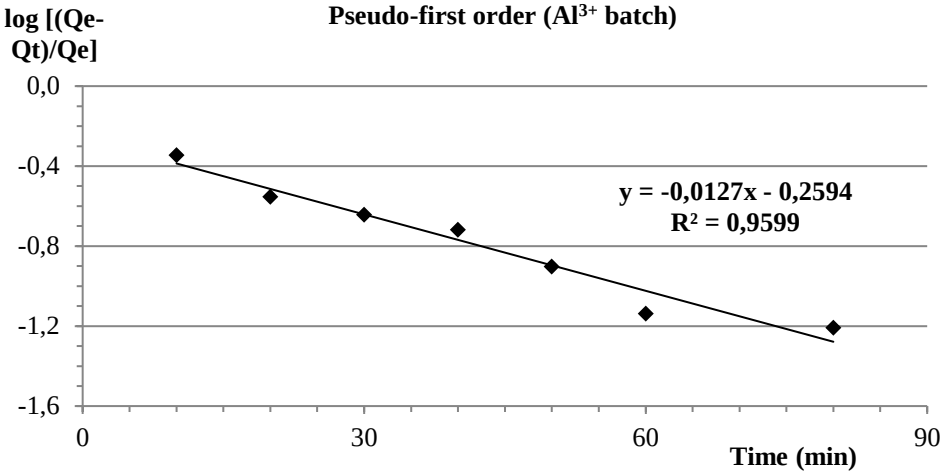

Next and using the pseudo-second order equation for the same process, the graph t/Q_t versus time was also obtained (Figure 10) and the experimental points fitted much better the theoretical linear model (R^2 = 0.9972).

Fig. 10. Graph of the experimental data (batch process for Al^{3+}) according to the pseudo-second order equation (n = 3).

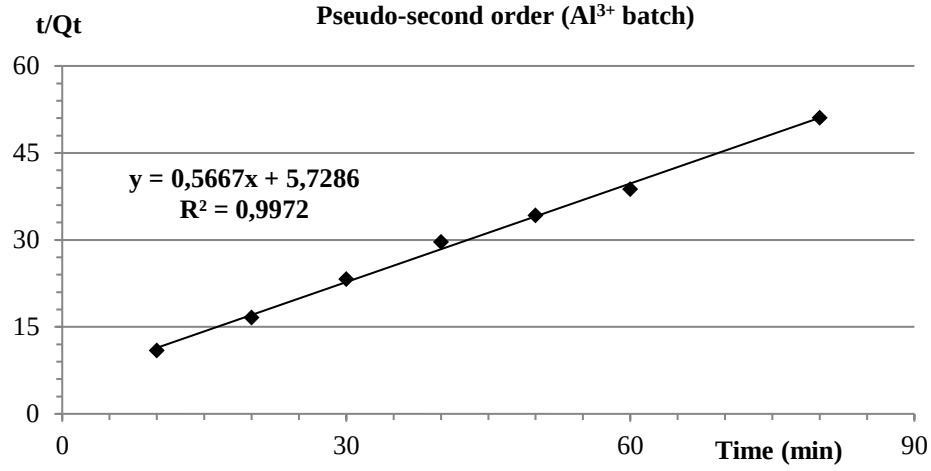

As the second-order model was more adequate to describe the batch process for Al^{3+}, this model was used to compare the experimental and theoretical values of Q_m, showing good agreement between them (Table 2). These two evidences (excellent adequacy to the linear experimental curve and

similarity between theoretical and actual values of Q_m) suggest that this process follows a pseudo-second order mechanism, and consequently is possible to assume that the chemisorption (formation of bonds between SCG and metal ions) is the rate-limiting step (Febrianto et al., 2009).

Finally, the free energy change (ΔG^o) of the batch process for Al^{3+} was determined using the equation

$$\Delta G^o = -RT \ln K_c' \qquad (11)$$

Were R = universal gas constant (8.314 J/mol.K), T = absolute temperature (293 K as experiments were done at 20 ºC) and K_c' = apparent equilibrium constant determine as C_e in the biossorbent / C_e in the solution at the equilibrium point (Sud et al, 2008). As calculated ΔG^o was negative (-6.07 kJ/mol) as shown in Table 2, this process tends to be thermodynamically favorable, confirming the conclusion found in item 3.4.1. using the parameter R_L.

Similar analysis were done for the other processes and ions evaluated in the present study (graphs not included) and the conclusions were consistent as all of them showed better adequacy to the second-order model, good correlation between $Q_{m(exp)}$ and $Q_{m(theo)}$ and negative values for ΔG^o (Table 2).

Table 2 Values of R^2 for different kinetic models, comparison of experimental and theoretical values of Q_m (mg/g SCG) and ΔG^o (kJ/mol) for the second-order model.

Process	R^2 (1st-order)	R^2 (2nd-order)	$Q_{m(exp)}$*	$Q_{m(theo)}$*	ΔG^o*
Batch Al^{3+}	0.960	0.997	3.12	3.35	-6.07
Batch Fe^{2+}	0.859	0.999	4.21	4.36	-4.41
Continuous Al^{3+}	0.966	0.997	1.79	1.81	-8.60
Continuous Fe^{2+}	0.841	0.985	3.34	2.99	-7.84

* Values obtained using the second-order model and solutions with 100 mg/L of Al^{3+} or Fe^{2+}.

4 CONCLUSIONS

The SCG showed to be an excellent material to remove Al^{3+} and Fe^{2+} from aqueous effluents using batch or continuous processes due to its efficiency and marginal cost. The parameters time of contact, agitation speed and mass of biosorbent were evaluated to determine the optimum conditions for each process.

The continuous process showed higher removal efficiency (capacity to remove the ions from the effluent) for both ions (items 3.2. and 3.3.) but the batch process was able to remove larger quantities of both contaminants per mass unit of SCG (item 3.4.). These conclusions agree with another study done with tea waste to absorb Cu^{2+} and Pb^{2+} using batch and fixed bed column (Amarasinghe & Williams, 2007).

The Langmuir-3 model proved to be the most accurate to describe the tests and the kinetic

evaluations indicated that all processes follow a second-order model, being thermodynamically favorable within the conditions covered along this study.

REFERENCES

Agbozu, I.E., Emoruwa, F.O., 2014. Batch adsorption of heavy metals (Cu, Pb, Fe, Cr and Cd) from aqueous solutions using coconut husk. Afr. J. Environ. Sci. Technol. 8, 239-246.

Amarasinghe, B.M.W.P.K., Williams, R.A., 2007. Tea waste as a low cost adsorbent for the removal of Cu and Pb from wastewater. Chem. Eng. J. 132, 299-309.

Azouaou, N., Sadaoui, Z., Djaafri, A., Mokaddem, H., 2010. Adsorption of cadmium from aqueous solution onto untreated coffee grounds: equilibrium, kinectics and thermodynamics. J. Hazard. Mater. 184, 126-134.

Baird, R.B., Eaton, A.D., Rice, E.W., 2017. Standard Methods for the Examination of Water and Wastewater, 23rd ed. American Public Health Association, Washington DC.

Chao, H.P., Chang, C.C., Nieva, A., 2014. Biosorption of heavy metals on *Citrus maxima* peel, passion fruit shell, and sugarcane bagasse in a fixed column. J. Ind. Eng. Chem. 20, 3408-3414.

Dávila-Guzmán, N.E., Cerino-Córdova, F.J., Soto-Regalado, E., Rangel-Mendez, J.R., Díaz-Flores, P.E., Garza-Gonzalez, M.T., Loredo-Medrano, J.A., 2013. Copper biosorption by spent coffee ground: equilibrium, kinetics, and mechanism. Clean Soil Air Water 41, 557-564.

Febrianto, J., Kosasih, A.N., Sunarso, J., Ju, Y.H., Indraswati, N., Ismadji, S., 2009. Equilibrium and kinetic studies in adsorption of heavy metals using biosorbent: A summary of recent studies. J. Hazard Mater. 162, 616-645.

Freundlich, H.M.F., 1906. Over the adsorption in solution. J. Phys. Chem. 57, 385-471.

Gao, X., Dai, Y., Zhang, Y., Fu, F., 2016. Effective adsorption of phenolic compound from aqueous solutions on activated semi coke. J. Phys. Chem. Solids 102, 142-150.

Hashim, M.A., Mukhopadhyay, S., Sahu, J.N., Sengupta, B., 2011. Remediation technologies for heavy metals contaminated groundwater. J. Environ. Manage. 92, 2355-2388.

Keng, P.S., Lee, S.L., Ha, S.T., Hung, Y.T., Ong, S.T., 2014. Removal of hazardous heavy metals from aqueous environment by low-cost adsorption materials. Environ. Chem. Lett. 12, 15-25.

Muslim,A., Abubakar, Alam, P. N., Usman, H., Randa, G., Widayat, A. H., Al Hakim, A. Y., Hadiba, T., 2022. Silicified coal adsorbents for adsorption of Cu(II) from the aqueous Solution: Non-Linear kinetic and isotherm studies. Mater. Today – Proc. In press.

Lakshmipathy, R., Sarada, N.C., 2013. Application of watermelon rind as sorbent of nickel and cobalt from aqueous solution. Int. J. Miner. Process. 122, 63-65.

Langmuir, I., 1916. The constitution and fundamental properties of solids and liquids. J. Am. Chem. Soc. 38, 2221-2295.

Revathi, M., Saravanam, M., Basha, A.M., Velan, M., 2012. Removal of copper, nickel and zinc ions from electroplating rinse water. Clean Soil Air Water 40, 66-79.

Wang,S., Wang, N., Yao, K., Fan, Y., Li, W., Han, W., Yin, X., Chen, D., 2019. Characterization and Interpretation of Cd (II) Adsorption by Different Modified Rice Straws under Contrasting Conditions. Sci Rep. 9, 17868.

Sathasivam, K., Haris, M.R.H.M., 2010. Banana trunk fibers as an efficient biosorbent for the removal

of Cd(II), Cu(II), Fe(II) and Zn(II) from aqueous solutions. J. Chil. Chem. Soc. 55, 278-282.

Ahn, J.Y., Kil, D.Y., Kong, C., Kim, B. G., 2014. Comparison of Oven-drying Methods for Determination of Moisture Content in Feed Ingredients. Asian-Australas J Anim Sci. 27 (11): 1615–1622.

Smith, D.W., 1977. Ionic hydration enthalpies. J. Chem. Educ. 54, 540-542.

Sousa, D.A., Oliveira, E., Nogueira, M.C., Espósito, B.P., 2010. Development of a heavy metal sorption system through the P=S functionalisation of coconut (*Cocos nucifera*) fibers. Bioresour. Technol. 101, 138-143.

Sud, D., Mahajan, G., Kaur, M.P., 2008. Agricultural waste material as potential adsorbent for sequestering heavy metal ions from solutions – A review. Biores. Technol. 99, 6017-6027.

Vijayaraghavan, K., Balasubramanian, R., 2015. Is biosorption suitable for the contamination of metal-bearing wastewater? A critical review on the state-of-the-art of biosorption processes and future directions. J. Environ. Manage. 160, 283-296.

Wang, C., Boithias, L., Ning, Z., Han, Y., Sauvage, S., Sánchez-Pérez, J.M., Kuramochi, K., Hatano, R., 2017. Comparison of Langmuir and Freundlich adsoption equations within the SWAT-K model for assessing potassium environmental losses at basin scale. Agric. Water Manage. 180, 205-211.

Witek-Krowiak, A., Szafran, R.G., Modelski, S., 2011. Biosorption of heavy metals from aqueous solutions onto peanut shell as a low-cost biosorbent. Desalination 265, 126-134.